ELSEVIER

Journal of Nuclear Materials 248 (1997) 1–8

journal of nuclear materials

Section 1. Fuel particle balance and dynamics in plasma facing materials

Physical sputtering and reflection processes in plasma–wall interactions

W. Eckstein *

EURATOM-Association, Max-Planck-Institut für Plasmaphysik, D-85748 Garching, Germany

Abstract

The current status of sputtering of and reflection from pure elements regarded as possible wall or divertor materials is reviewed for the bombardment with hydrogen isotopes and self-ions. The general behavior of sputtering and reflection on the projectile energy and angle of incidence as well as surface roughness is discussed. But in a fusion machine the atoms bombarding the walls and divertor plates have a broad energy and angular distribution. Therefore, computer simulation allows to study the dependence on a Maxwellian projectile distribution as a function of the edge plasma temperature which may be a more relevant description of the situation in a plasma machine. The case of multicomponent targets is more difficult and each system has to be studied individually. Preferential sputtering, usually the preferred emission of the lighter target species, changes the surface composition. Therefore, only a few examples will demonstrate the change of surface composition, sputtering and reflection, and depth profiles with fluence (time). Simultaneous bombardment with more than one species complicates further the situation, where an erosion dominated regime can change into a deposition dominated regime with time. © 1997 Elsevier Science B.V.

1. Introduction

Physical sputtering is one of the most serious processes of erosion of the innermost surfaces of fusion machines. Backscattering or reflection of plasma atoms contribute to the recycling of hydrogen and the backscattering of impurity species can be of importance in some cases.

The most important elemental species of wall material are the light elements Be, B, and C either in the form of tiles covering the metal vessel or by evaporating procedures of boronization and carbonization. In future machines as ITER heavy elements as W are considered, too. Hydrogen isotopes form the largest fluxes to the surfaces, but impurity species as C and O cannot be neglected, and nearly all eroded wall species will return to the wall. Gases as N_2, Ne and Ar are used and considered in ITER as a means of radiation cooling in the divertor. Furthermore, He as the reaction product in the fusion process will always be present and can have still high energies when reaching the surface. Metal atoms as Fe and Ni from the vessel wall may be of less importance due to the coverage of the wall with other materials.

This paper will, therefore, concentrate on results for elemental species mentioned above which are relevant in fusion machines. As indicated in the title this paper deals with the physical processes, which means it considers the processes which can be described by collisional processes. Chemical effects as chemical erosion, for example, are not discussed in this paper.

On a microscopic scale the processes of ion bombardment of solids can be described in the following way: An incoming particle, neutral or charged, will penetrate the target. It looses energy due to collisions with target atoms (elastic energy loss) and target electrons (electronic or inelastic energy loss). In an elastic collision the direction of the moving atom is also changed which is not the case for inelastic collisions. In an elastic collision enough energy can be transferred to a target atom that it also starts to move, a recoil is created. This can happen again and in addition the recoil can generate additional recoils, so that a cascade of moving atoms is created. If the incoming atom leaves the surface after some scattering events, one talks

* Corresponding author. Tel.: +49-89 3299 1259; fax: +49-89 3299 1149; e-mail: wge@ipp-garching.mpg.de.

0022-3115/97/$17.00 © 1997 Elsevier Science B.V. All rights reserved.
PII S0022-3115(97)00109-8

about backscattering or reflection. If a target atom gets enough energy to overcome the surface barrier and escapes the target, then this process is called sputtering.

Data on sputtering and backscattering can be obtained by experiments, but also by computer simulation [1] and the analytic theory [2]. Here we concentrate on experimental data and values determined by computer simulations based on the binary collision approximation (BCA). Relevant overviews are given in Refs. [3–6].

2. Sputtering

2.1. Yields

A collection of older experimental data is given by Andersen and Bay [7–9], newer experimental and calculated values by Thomas et al. (should be used with some care) [10] and by Eckstein et al. [11]. The energy dependence of the sputter yield Y at normal incidence, $\alpha = 0°$, can be described by an analytic formula [11,12], the Bohdansky formula [13]

$$Y(E_0, \alpha = 0°) = Q s_n(\varepsilon)\left(1 - \left(\frac{E_{th}}{E_0}\right)^{2/3}\right)\left(1 - \frac{E_{th}}{E_0}\right)^2, \tag{1}$$

which is based on the analytic theory [2]. Eq. (1) contains two parameters Q and E_{th}. Q adjusts the curve to the maximum sputter yield and E_{th} is the sputter threshold. $s_n(\varepsilon)$ is the elastic stopping based on the KrC potential

$$s_n(\varepsilon) = \frac{\ln(1 + 1.2288\varepsilon)}{2(\varepsilon + 0.008\varepsilon^{0.1504} + 0.1728\sqrt{\varepsilon})} \tag{2}$$

as a function of the reduced energy ε,

$$\varepsilon = E_0 \frac{M_2}{M_1 + M_2} \frac{0.03254}{Z_1 Z_2 (Z_1^{2/3} + Z_2^{2/3})^{1/2}}, \tag{3}$$

where Z_1, Z_2 and M_1, M_2 are the atomic numbers and the masses of the incident and target atom, respectively. E_0 is the energy (in eV) of the incident atom. Eq. (1) may provide too low values near the threshold. Yamamura [14] gives a slightly more complicated formula for the yield by including some refinements.

A formula for the dependence of the sputter yield on the angle of incidence was given by Yamamura et al. [15]

$$Y(E_0, \alpha) = Y(E_0, \alpha = 0°)(\cos\alpha)^{-f} \exp\left\{f\left[1 - (\cos\alpha)^{-1}\right]\sin\eta\right\}. \tag{4}$$

The fitting parameters f and $\eta = \pi/2 - \alpha_m$ can be found in Refs. [11,15] for some examples; α_m is the angle at which the sputter yield reaches its maximum. Yamamura et al. [15] give analytic formulae for f and η which are both not independent of the incident energy E_0 [11]. Eq. (4) is not applicable at low energies for heavy incident atoms.

Many calculated sputter yields are given in [14,16] for elemental targets and in [17] for B_4C. Ref. [11] provides experimental and calculated values for monoatomic targets as well as for some compounds. Tables of sputter yields, Y, and sputtered energies, Y_E, as a function of incident energy and angle of incidence have been calculated by Eckstein as input data for plasma edge codes. Tables exist so far for H, D, T, He, C, N, Ne, and Ar on C and for H, D, T, He, N, Ne, Ar, and W on W. Most values are given for 10 to 1000 eV and for 0° to 85°. These values are accessible from /afs/ipp/u/wge/trim.data/sputter.data. An example is shown in Fig. 1. New experimental data for yields of Be self-sputtering are reported in Refs. [18,19].

2.2. Sputtering threshold

The condition for an atom to be sputtered is that it must have enough energy to overcome the planar surface potential which causes an energy loss and a refraction towards the surface. Therefore, W with the highest surface binding energy of all elements and a large mass ratio (M_2/M_1) has a high threshold for hydrogen and explains the interest in that metal for fusion machines. As shown in Ref. [20] for large mass ratios the threshold energy for sputtering is nearly independent on the angle of incidence which is not the case for low mass ratios. In this case the threshold energy decreases with the angle of incidence which is especially important for impurity sputtering at the inner walls. An empirical formula for the threshold energy, E_{th}, at normal incidence is given in [12]

$$\frac{E_{th}}{E_s} = 7.0\left(\frac{M_2}{M_1}\right)^{-0.54} + 0.15\left(\frac{M_2}{M_1}\right)^{1.12}. \tag{5}$$

E_s is the surface binding energy (heat of sublimation). For low mass ratios ($M_2/M_1 \le 5$) the threshold energy can be a factor of three to five lower at grazing incidence than for normal incidence [20]. In Ref. [20] other threshold formulae for normal incidence available in the literature are given.

2.3. Energy and angular distributions

Measured energy distributions of sputtered atoms show a maximum close to half the surface binding energy, which is also the case for calculated energy distributions, if a planar surface potential is applied [1]. The analytic theory gives a value of $E_s/(2 - 2m)$ for the position of the maximum [2] which leads to $0.6E_s$ for a reasonable value $m = 1/6$ in the exponent of the power potential. All experimentally determined distributions are measured in a small solid angle. Computer simulation shows that the form of the distribution depends on the exit angle [21], an effect which is generally neglected. With an increasing angle of incidence the maximum position does practically

not change, although the number of high energy direct recoils increases which results in an increase of the mean energy of sputtered atoms. The mean energy also increases with increasing incident energy due to the shift of the high energy end of the distribution to higher energies. It can be determined by $E_{mean} = E_0 Y_E / Y$.

The angular distribution of sputtered atoms is in a first approximation a cosine distribution, but with a tendency for an overcosine distribution (more intensity in the direction of the surface normal) at higher incident energies and for an undercosine at low incident energies [1]. At large angles of incidence the direct recoils are emitted predominantly in the forward direction. Although these direct recoils can easily be measured in the plane of incidence, they constitute only a small fraction of all sputtered atoms [22].

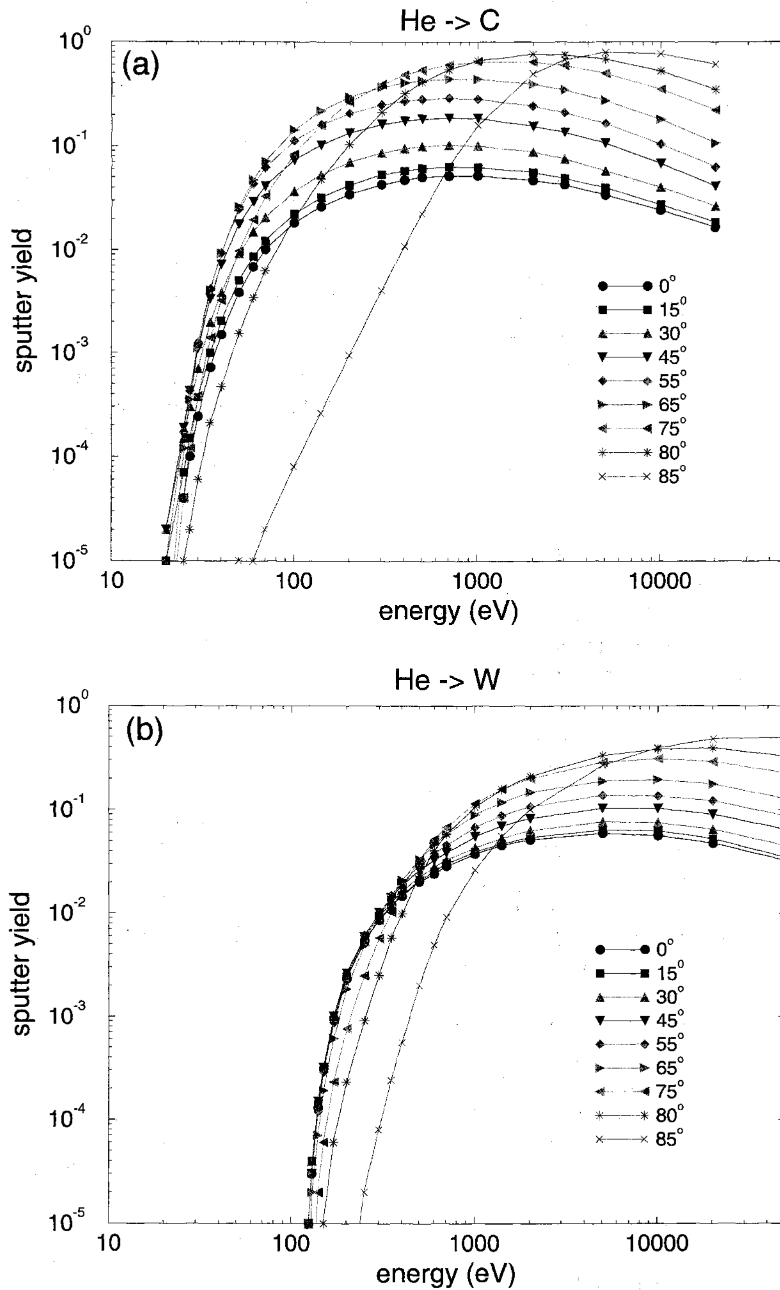

Fig. 1. Sputter yields for several angle of incidence versus the incident energy for (a) He on C and (b) He on W.

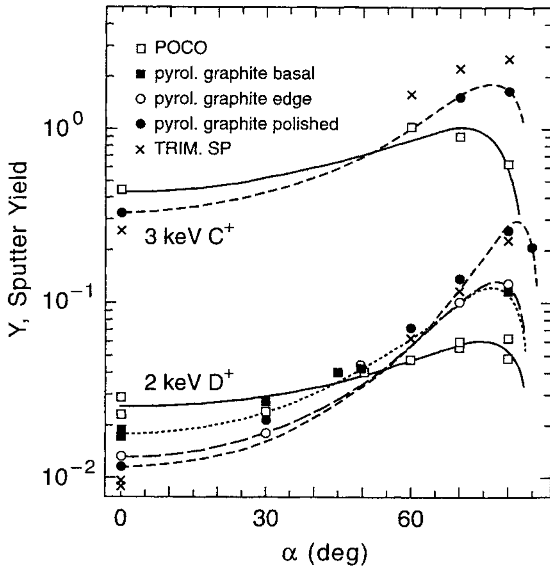

Fig. 2. Sputter yield, Y, versus the angle of incidence, α, for the bombardment of different types of graphite with 2 keV D and 3 keV C. Experimental data for POCO, pyrol. graphite basal, pyrol. graphite edge, and pyrol. graphite polished (decreasing roughness) are compared with results from computer simulation (TRIM.SP) (from fig. 5 of Ref. [4]).

2.4. Surface roughness, excited and molecular states

Surface roughness is important, because it can change the effective sputter yields up to a factor of 5, as shown in Fig. 2. Generally, the yield is reduced at large angles of incidence and increased at normal incidence. This experimental result can be understood by the fact that for a nominally normal incidence the incoming atoms hit the rough surface effectively at oblique angles of incidence, the opposite effect will happen for a nominally oblique incidence. The effect of redeposition of sputtered atoms may also play a role. Most computed sputter yield values are determined for nearly flat surfaces, whereas most experimental data come from rough surfaces. Therefore, deviations are not surprising. Ruzic [23] has applied the fractal concept into simulations and even studied the development of roughness by ion bombardment [24]. The problem is that one is not sure that all rough or even most surfaces can be described by a fractal geometry.

Most sputtered atoms are not in an excited state (includes the ionic state), but even a small fraction of excited atoms may not be neglected, because they may be more easily ionized in the edge plasma. Molecular sputtered species are known, but again their fraction is small in most cases.

2.5. Incident Maxwellian distribution

So far only mono-energetic bombardment has been discussed, but in a fusion plasma machine atoms with a broad energy distribution arrive at surfaces. This problem is hard to address in a laboratory experiment, but it can be handled by computer simulation. The most reasonable assumption is a Maxwellian distribution including a sheath potential in front of the surface. The sheath potential increases the energy of the ions (increasing the yield) and decreases the angle of incidence (decreases the yield). Multicharged impurity species are accelerated more strongly in the sheath and will increase the sputter yield. Therefore, a low plasma edge temperature is essential to reduce sputtering. Examples can be found in figs. 11–13 of Ref. [6].

2.6. Multicomponent systems

In this section fall all multicomponent targets as well as monoatomic targets, which are bombarded with a nonvolatile species, and targets which are bombarded simultaneously by several species. This is the most general case and probably the most common in plasma machines. Some systems as carbides can be treated purely collisional, but at higher temperatures diffusion and segregation effects have to be taken into account. Generally, the composition will be changed in the implantation range of the incident atom and this change depends on time or fluence until some kind of equilibrium is reached. In a target material with several isotopes the surface layers will enrich in the heavy isotope due to the preferential sputtering of the light isotopes, for example. Each system has to investigated specifically.

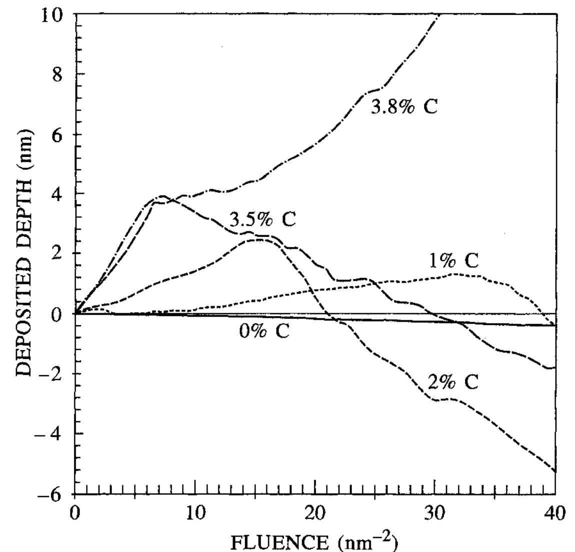

Fig. 3. Deposition and erosion versus the incident fluence. W is bombarded simultaneously with D and C^{3+} as an impurity assuming a Maxwellian distribution, a plasma edge temperature $T_e = 40$ eV and a sheath potential of $3kT$. Curves are calculated with TRIDYN [28].

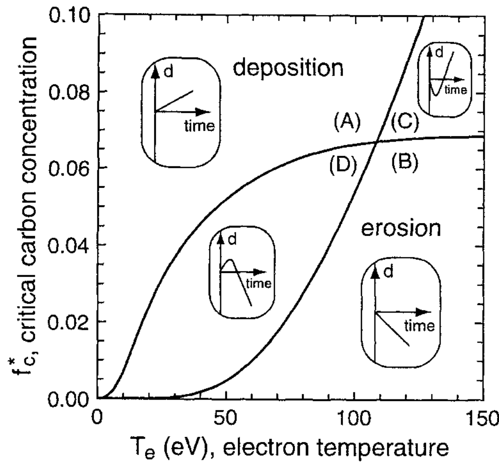

Fig. 4. The critical concentration f_c^* at which deposition behavior changes into erosion versus the plasma edge temperature T_e. W is bombarded simultaneously with D and C^{3+} as an impurity assuming a Maxwellian distribution and a sheath potential of $3kT$. Schematically indicated are the four possible time developments in their region of validity (from fig. 7 of Ref. [27]).

One example discussed in Ref. [25] is the bombardment of W with C. Experiments and simulations clearly show, that deposition of C occurs at normal incidence and erosion at large angles of incidence. At intermediate angles deposition switches to erosion and large fluences are needed to reach a steady state. Deposition means that with increasing C fluence (or bombardment time) layers of C at the surface will increase in thickness, because C self-sputtering stays below unity for normal incidence. If erosion dominates a steady state or equilibrium is reached leading to a mixed composition profile in the implantation range.

Another, more close to actual conditions in a plasma machine, example is the bombardment of a monoatomic target with a Maxwellian distribution of D and C^{3+} at a fixed plasma edge temperature [26,27]. As demonstrated in Fig. 3 deposition of C or erosion depends strongly on the incoming impurity concentration and on the fluence. Above some impurity concentration deposition is always observed. Fig. 4 shows at which impurity concentration and plasma temperature only deposition (A) or erosion (B) occurs, and where at first erosion and then deposition (C) or at first deposition and then erosion (D) will happen. These results are obtained neglecting diffusion and segregation.

3. Backscattering

The backscattered hydrogen contributes to the recycling of hydrogen in the plasma machine. In contrast to sputtered or thermally desorbed species backscattered hydrogen can retain an appreciable fraction of their incident energy which allows them to penetrate deeper into the plasma. Reflected heavy species have usually similar energies as sputtered atoms but they can outnumber sputtered atoms under some conditions.

3.1. Reflection coefficients

There are several reviews around which have collected the available data at the time of publication [3,5,29–38]. The most recent comprehensive data collection and their representation in fit formulae is given in Refs. [37,38]. The particle and energy reflection coefficients, R_N and R_E, at normal incidence can be fitted by the following formula:

$$R_N(\text{or } R_E) = \frac{A_1 \ln(A_2\varepsilon + e)}{1 + A_3\varepsilon^{A_4} + A_5\varepsilon^{A_6}} + A_7 \ln\left(\frac{A_8}{\varepsilon} + e\right). \tag{6}$$

The second term in Eq. (7) is only necessary for $\varepsilon > 40$. The fitting parameters A_i, different for R_N and R_E, are only valid for some mass ratio (M_2/M_1) range. An example for the particle reflection coefficient and different mass ratios is given in Fig. 5. Another example shows the particle reflection coefficients for the hydrogen isotopes and helium on C and W as a function of energy in Fig. 6. It clearly demonstrates the increase of the particle reflection coefficient with increasing mass ratio. For self-ion bombardment the surface binding potential accelerates the incoming atom and decelerates the backscattered atom with the result that the reflection coefficients decrease at low energies [39] in contrast to noble gas ion bombardment or in cases with very low binding energies. This effect is shown in Fig. 7. It can be described by a similar formula as above [37,38]:

$$R_N(\text{or } R_E) = \frac{A_1 \ln(A_2\varepsilon + e)}{1 + A_3\varepsilon^{A_4} + A_5\varepsilon^{A_6}} \left[\left(1 - \frac{A_7}{\varepsilon}\right)^{A_8}\right]^{A_9}. \tag{7}$$

Eqs. (6) and (7) are simpler than those given in Ref. [34]. All the data recommended in Refs. [37,38] are stored in the ALADDIN data base of the atomic and molecular data unit of the IAEA and can be retrieved from there.

Experimental data for heavy ion reflection and for light ion reflection at low energies are very scarce. Most of the knowledge relies on computed values. The relevant literature is given in Ref. [5]. Below 30 eV only a few experimental reflection coefficients exist for the backscattering of D from W [40].

Very limited is also the availability of experimental reflection coefficients for oblique incidence. Recently only one paper gave experimental and calculated values for R_N for D on two different kind of graphites at relative low energies [41]. The results are shown in Fig. 8. Again, computer calculations are the fastest way to get reliable

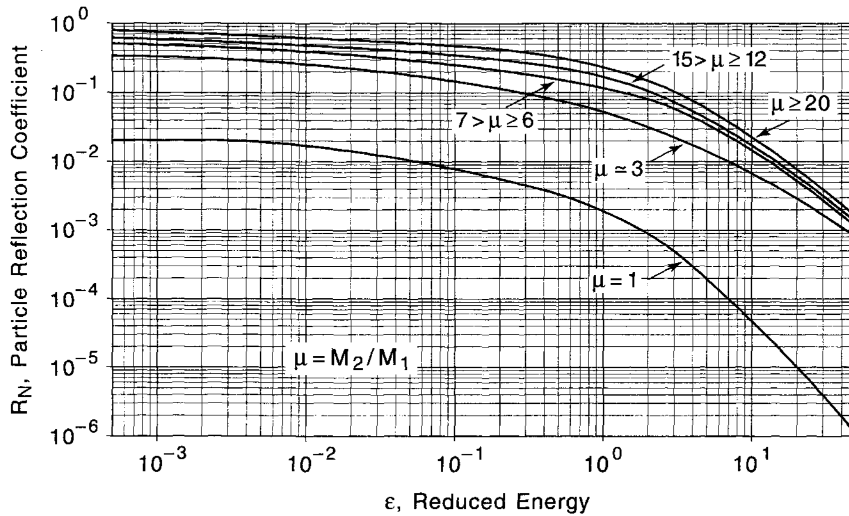

Fig. 5. The particle reflection coefficient, R_N, versus the reduced energy, ε, for different mass ratios $\mu = M_2/M_1$ and normal incidence (from fig. 6 of Ref. [37]).

values. As in the case for sputtering reflection coefficients, R_N and R_E, have been determined for the same combinations as a function of incident energy and angle. These values are accessible from /afs/ipp/u/wge/trim.data/refl.data. The results show clearly that for self-bombardment reflection is more important than sputtering for large angles of incidence. New calculated values of R_N for light ions are given in Ref. [42]. Composite targets may be handled by using an average charge and mass [3,37].

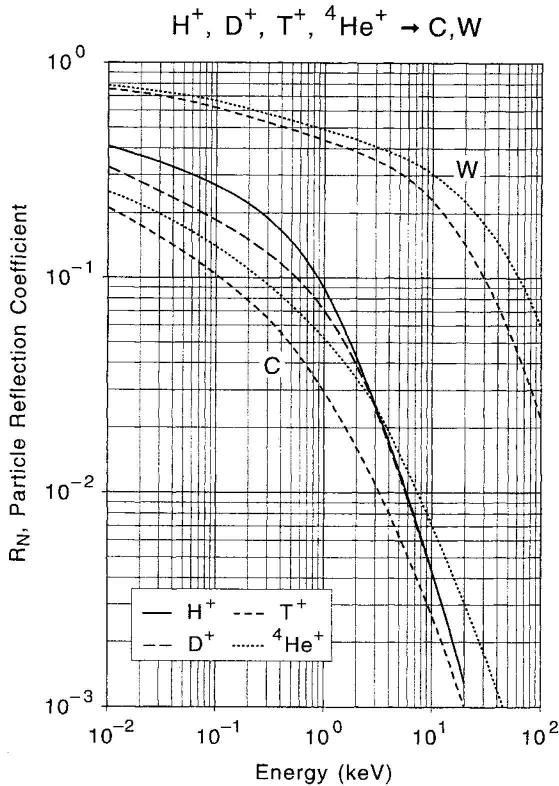

Fig. 6. The particle reflection coefficient, R_N, versus the incident energy, E_0, at normal incidence for the hydrogen isotopes and ^{4}He on C and W targets (from Ref. [37]).

3.2. Energy and angular distributions

In contrast to sputtering the energy distributions of backscattered atoms extend to larger energies, in general. Especially for hydrogen and large mass ratios, the highest energies are close to the incident energy due to backscattering from surface atoms. This is even more pronounced at oblique incidence. It also means that the mean energy of reflected atoms is usually higher than in sputtering. It can be determined by $E_{\text{mean}} = E_0 R_N / R_E$. Valuable information can be found in [3,5].

As in sputtering the angular distribution of backscattered atoms is close to a cosine distribution, but at oblique angles of incidence the atoms are reflected in the forward direction until at some grazing incidence nearly specular reflection (although broadened) is attained. Computer results give these distributions in some reduced way as an input for plasma codes [43–45].

3.3. Surface roughness, excited states

Surface roughness is important for reflected particles as for sputtered atoms. Experimental data [41] show that the effect on the particle reflection coefficient increases with the angle of incidence (lowering the reflection coefficient) and decreases with the incident energy as one would expect. Where it applies the fractal concept for a rough surface in a simulation [41,46] seems to work well.

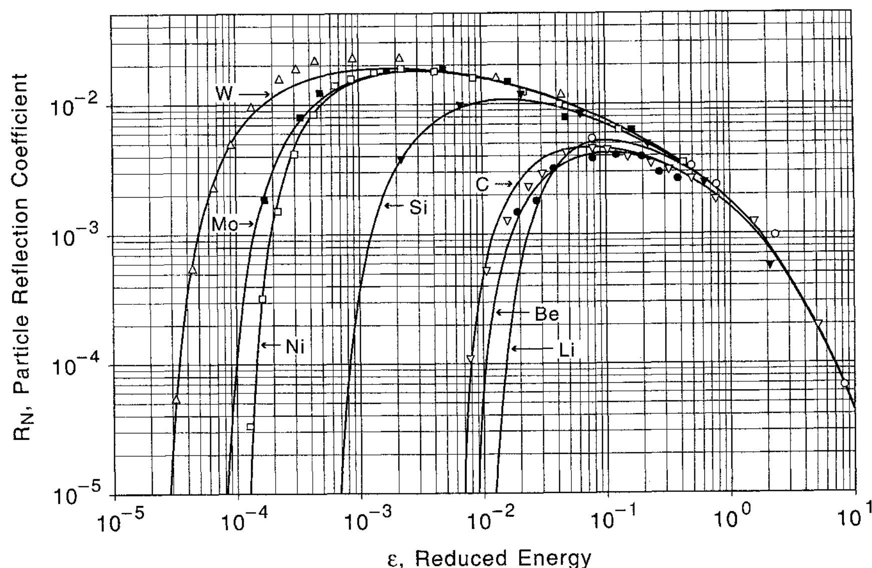

Fig. 7. The particle reflection coefficient, R_N, versus the reduced energy, ε, for self-bombardment ($\mu = M_2/M_1 = 1$) and normal incidence (from fig. 13 of Ref. [37], symbols are calculated values from Ref. [39]).

Similar as in sputtered species excited and ionized states do not play an important role. For hydrogen, neutral as well as positive and negative charge states are found [3], but below 1 keV the neutral fraction is larger than 90% and nearly independent on the target material. H_α emission from reflected hydrogen is reported in Ref. [47].

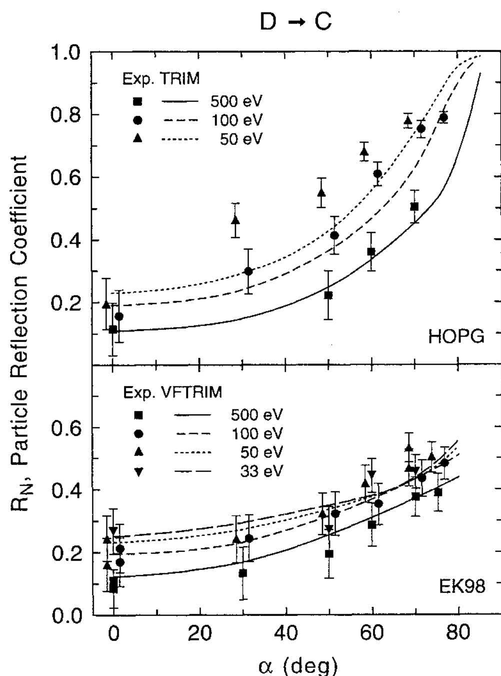

Fig. 8. The particle reflection coefficient, R_N, versus the angle of incidence, α. HOPG (top) and EK98 (bottom) are bombarded with D at several energies. Experimental data (symbols) are compared with computed results (lines) using TRVMC (top) and VFTRIM (bottom) applying a fractal dimension of 2.05 determined experimentally (from fig. 10 of Ref. [41]).

4. Conclusions

The data base for sputtering is in relative good shape, at least for normal incidence. Computer simulation has been shown to be a good complement to the often time consuming measurements. The influence of surface roughness still awaits a systematic treatment. Measurements near the threshold are scarce due to experimental difficulties.

As in sputtering the database for reflection at normal incidence is quite substantial, but for oblique incidence and heavy particle reflection the experimental basis is very small.

References

[1] W. Eckstein, Computer Simulation of Ion-Solid Interactions, Springer Series in Materials Science, Vol. 10 (Springer, Berlin, 1991).

[2] P. Sigmund, in: Sputtering by Particle Bombardment I, ed. R. Behrisch, Topics Appl. Phys., Vol. 47 (Springer, Berlin, 1981) p. 9.

[3] R.A. Langley, J. Bohdansky, W. Eckstein, P. Mioduszewski, J. Roth, E. Taglauer, E.W. Thomas, H. Verbeek, K.L. Wilson, Data Compendium for Plasma–Surface Interactions, Nucl. Fusion, Special Issue, 1984 (IAEA, Vienna, 1984).

[4] W. Eckstein, J. Bohdansky, J. Roth, Atomic and Plasma–Material Interaction Data for Fusion, Supplement to Nucl. Fusion, Vol. 1 (IAEA, Vienna, 1991) p. 51.

[5] W. Eckstein, Atomic and Plasma–Material Interaction Data for Fusion, Supplement to Nucl. Fusion, Vol. 1 (IAEA, Vienna, 1991) p. 17.
[6] W. Eckstein, V. Philipps, in: Physical Processes of the Interaction of Fusion Plasmas with Solids, eds. W.O. Hofer and J. Roth (Academic Press, San Diego, CA, 1996) p. 93.
[7] H.H. Andersen, H.L. Bay, in: Sputtering by Particle Bombardment I, ed. R. Behrisch, Topics Appl. Phys., Vol. 47 (Springer, Berlin, 1981) p. 145.
[8] N. Matsunami, Y. Yamamura, Y. Itikawa, N. Itoh, Y. Kazumata, S. Miyagawa, K. Morita, R. Shimizu, H. Tawara, At. Data Nucl. Data Tables 31 (1984) 1.
[9] Y. Yamamura, Y. Mizuno, IPPJ-AM-40, Nagoya, Japan, 1985.
[10] E.W. Thomas, R.K. Janev, J. Botero, J.J. Smith, Y. Qiu, INDC(NDS) 287, IAEA, Vienna 1993.
[11] W. Eckstein, C. Garcia-Rosales, J. Roth, W. Ottenberger IPP-report 9/82, Garching, FRG, 1993.
[12] C. Garcia-Rosales, W. Eckstein, J. Roth, J. Nucl. Mater. 218 (1994) 8.
[13] J. Bohdansky, Nucl. Instrum. Methods B2 (1984) 587.
[14] Y. Yamamura, H. Tawara, NIFS-DATA-23, Nagoya, Japan, 1995.
[15] Y. Yamamura, Y. Itikawa, Y. Itoh, IPPJ-AM-26, Nagoya, Japan, 1983.
[16] Y. Yamamura, K. Sakaoka, H. Tawara, NIFS-DATA-31, Nagoya, Japan, 1995.
[17] T. Ono, T. Kawamura, K. Ishii, Y. Yamamura, NIFS-DATA-34, Nagoya, Japan, 1996.
[18] E. Hechtl, J. Roth, W. Eckstein, C.H. Wu, J. Nucl. Mater. 220–222 (1995) 883.
[19] M.I. Guseva, V.M. Gureev, S.N. Korshunov, V.E. Neumoin, Yu.A. Sokolov, V.G. Solyarova, V.I. Vasiliev, S.V. Rylov, V.M. Strunnikov, J. Nucl. Mater. 220–222 (1995) 957.
[20] W. Eckstein, C. Garciia-Rosales, J. Roth, J. Laszlo, Nucl. Instrum. Methods B83 (1993) 95.
[21] W. Eckstein, Nucl. Instrum. Methods B27 (1987) 78.
[22] W. Eckstein, Nucl. Instrum. Methods B18 (1987) 344.
[23] D.N. Ruzic, Nucl. Instrum. Methods B47 (1990) 118.
[24] M.A. Shaheen, D.N. Ruzic, J. Vac. Sci. Technol. A11 (1993) 3085.
[25] W. Eckstein, J. Roth, Nucl. Instrum. Methods B53 (1991) 279.
[26] D. Naujoks, W. Eckstein, J. Nucl. Mater. 220–222 (1995) 993.
[27] D. Naujoks, W. Eckstein, J. Nucl. Mater. 230 (1996) 93.
[28] W. Möller, W. Eckstein, J. Biersack, Comput. Phys. Commun. 51 (1988) 355.
[29] W. Eckstein, H. Verbeek, IPP-report 9/32, Garching, FRG, 1979
[30] T. Tabata, R. Ito, Y. Itikawa, N. Itoh, K. Morita, IPPJ-AM 18, Nagoya, Japan, 1981
[31] T. Tabata, R. Ito, Y. Itikawa, N. Itoh, K. Morita, At. Data Nucl. Data Tables 28 (1983) 493.
[32] T. Tabata, R. Ito, Y. Itikawa, N. Itoh, K. Morita, H. Tawara, IPPJ-AM 34, Nagoya, Japan, 1984.
[33] K. Morita, T. Tabata, R. Ito, J. Nucl. Mater. 128&129 (1984) 681.
[34] R. Ito, T. Tabata, N. Itoh, K. Morita, T. Kato, H. Tawara, IPPJ-AM 41, Nagoya, Japan, 1985.
[35] T. Tabata, R. Ito, K. Morita, H. Tawara, Nucl. Instrum. Methods B9 (1985) 113.
[36] T. Tabata, R. Ito, K. Morita, H. Tawara, Radiat. Eff. 85 (1985) 45.
[37] E.W. Thomas, R.K. Janev, J.J. Smith, INDC(NDS)-249, IAEA, Vienna, 1991
[38] E.W. Thomas, R.K. Janev, J.J. Smith, Nucl. Instrum. Methods B69 (1992) 427.
[39] W. Eckstein, J.P. Biersack, Z. Phys. B63 (1986) 109.
[40] V.V. Bandurko, V.A. Kurnaev, Vacuum 44 (1993) 937.
[41] M. Mayer, W. Eckstein, B.M.U. Scherzer, J. Appl. Phys. 77 (1995) 6609.
[42] N.N. Koborov, V.A. Kurnaev, D.V. Levchuk, A.A. Pisarev, V.M. Sotnikov, O.V. Zabeida, V.I. Pistunovich, J. Nucl. Mater. 220–222 (1995) 953.
[43] W. Eckstein, D.B. Heifetz, IPP-report 9/59, Garching, FRG, 1986.
[44] W. Eckstein, D.B. Heifetz, J. Nucl. Mater. 145–147 (1987) 332.
[45] D. Reiter, W. Eckstein, G. Giesen, H.J. Belitz, Report Jül-2605, Jülich, FRG, 1992.
[46] D. Ruzic, H. Chiu, J. Nucl. Mater. 162 (1989) 904.
[47] T. Tanabe, K. Ohya, N. Otsuki, J. Nucl. Mater. 220–222 (1995) 841.